



Removal of Selected Azo Dyes and Phenolic Compounds via Tyrosinase Immobilized Magnetic Iron Oxide Silver Nanoparticles

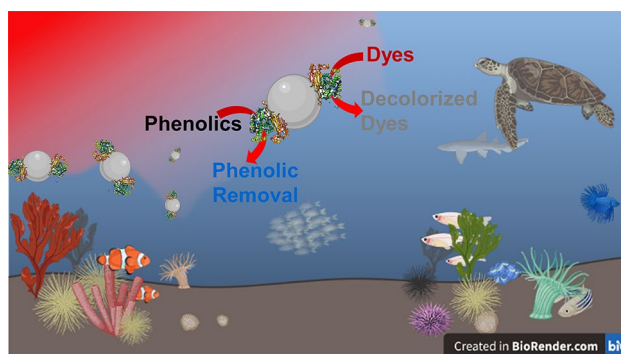
Rukiye Yavaşer¹ · Deniz Aktaş Uygun¹ · Arife Alev Karagözler¹

Received: 26 April 2022 / Accepted: 10 June 2022 / Published online: 1 July 2022
© The Author(s), under exclusive licence to Springer Science+Business Media, LLC, part of Springer Nature 2022

Abstract

Tyrosinase is a well-known oxidoreductase for removal of dyes and phenolic compounds regarded as hazardous and toxic substances concerning environmental issue and health of living systems. To develop an efficient, practical and reusable biocatalyst to remove these pollutants, covalent immobilization of *Agaricus bisporus* tyrosinase onto 3-mercaptopropionic acid modified silver-coated Fe₃O₄ nanoparticles through EDC/NHS chemistry was employed. Characterization techniques involving Fourier transform infrared spectroscopy, transmission electron microscopy–energy dispersive X-ray mapping and electron spin resonance confirmed the synthesis and immobilization success. The amount of immobilized tyrosinase was calculated to be 216.6 ± 1.250 mg per one gram of nanoparticles. Enzymatic characterization of free and immobilized tyrosinase was elucidated using two substrates, L-catechol and L-tyrosine to evaluate the differences in enzyme behavior towards different substrates. Optimum pH was 7.0 and 6.5 with L-catechol and L-tyrosine, respectively, for free and immobilized enzyme. Optimum temperatures were determined to be 45 °C and 35 °C for free and immobilized tyrosinase with L-catechol respectively, whereas with L-tyrosine, maximum activity was observed at 45 °C for both forms of tyrosinase. The affinity between tyrosinase and the substrates increased about 1.4 fold after immobilization. Immobilized tyrosinase preserved 48.9% of its initial activity after six reuses. Residual activity of immobilized tyrosinase was 68.3% after 84 days of storage whereas it was only 45.8% for free enzyme. Immobilized tyrosinase was able to decolorize azo dyes [Reactive Green 19 (36.9%) and Congo Red (95.0%)] and remove phenolic compounds [phenol (82.5%), Bisphenol F (65.0%), Bisphenol A (39.3%), *p*-cresol (73.1%), phenyl acetate (92.3%), 3-chlorophenol (50.5%), 4-chlorophenol (87.8%)] from aqueous solutions. Electrochemical behavior of immobilized tyrosinase as a catechol biosensing material was also demonstrated by cyclic voltammetry (CV). This work contributes to the bioremediation strategies that could be applied for removal of azo dyes and phenolic compounds from wastewaters through an environmentally-safe manner.

Graphical Abstract



Keywords Tyrosinase · Magnetic nanoparticles · Immobilization · Phenolic compounds · Dye removal

✉ Rukiye Yavaşer
ryavaser@adu.edu.tr

Extended author information available on the last page of the article

1 Introduction

Aquatic environment has been exposed to deterioration due to various industrial activities that release several hazardous compounds such as phenolic compounds, dyes, oil and grease toxic to living organisms [1, 2]. Presence of dyes and phenolic compounds in water has been a serious environmental concern due to their toxicity, carcinogenicity, poor biodegradability and persistence [3, 4]. Although existing methods including adsorption, extraction, chemical oxidation, Fenton oxidation and electrochemical treatments are applied, new and greener techniques are developed to overcome that global problem [4, 5]. Enzymatic bioremediation appears as a mild, efficient, low-cost and ecofriendly way compared to conventional methods [6].

Catalysis in living organisms is facilitated by enzyme molecules. Enzymatic reactions take place under mild conditions with excellent stereo-, regio- and chemoselectivity [7]. Adapting enzymes for *in vitro* catalysis opens the gate to employ a greener, efficient and practical strategy in various processes such as pharmaceutical, textile, food, pulp and paper, and waste treatment [8]. Since high cost, operational stability, recovery and reuse of free enzymes limit their usage, these drawbacks can be overcome by immobilization [9]. Immobilization of enzymes is defined as to fix enzyme molecules in a certain region or to bind them on a support material by different interactions generally classified as covalent attachment, entrapment, adsorption or cross-linking [10, 11]. The choice of enzyme-support interaction, chemical and physical properties of support material and characteristics of enzyme molecule are the key factors to develop a proper enzyme-immobilized system with high activity, stability and reusability [11]. Research on immobilization which started with the immobilization of invertase onto charcoal by Nelson and Griffin [12], is still developing by studies with various support materials, immobilization methods and enzymes. Magnetic nanoparticles, mainly Fe_3O_4 , have been widely employed for enzyme immobilization. Advantageous properties of these materials include response to magnetic field therefore easy separation from the products and recovery, surface modification, high surface area, and low mass transfer resistance [1, 13, 14].

One of the versatile enzymes that has been studied for immobilization is tyrosinase (TYR). Tyrosinase (E.C.1.14.18.1; monophenol monooxygenase) is a copper-containing oxidoreductase with a molecular mass of 119.5 kDa and isoelectric point of pH 4.7–5.0 [15]. Tyrosinase has bifunctional activity by catalyzing ortho-hydroxylation of monophenols to diphenols through cresolase activity and sequential oxidation of diphenols to quinones through catecholase activity [16, 17]. Due to

its broad substrate spectrum including a variety of phenolic compounds (e.g., L-tyrosine, L-3,4-dihydroxyphenyl alanine, catechol, caffeic acid, tyramine, phenol, *p*-aminophenol, cresol, *p*-cresol, dopamine, 4-hydroxyanisole, 4-butylcatechol, and pyrogallol) [18] and bifunctional activity, tyrosinase deserves increasing interest and applications in industry, building up biosensors and bioremediation of phenolic contaminants [17]. Free tyrosinase and tyrosinase-immobilized systems have been reported to be able to remove dyes such as methyl orange, Congo Red, Reactive Red 222, Reactive Blue 222, Reactive Yellow 39, Acid Orange 67 and Direct Blue 86 [19–21].

Considering the increasing environmental pollution as a result of dyes and phenolic compounds, production of a tyrosinase-immobilized nanoparticle system was aimed to remediate polluted water in this study. Since immobilization allows to obtain robust, reusable, easy-separable and economic enzymatic remediates, commercial tyrosinase was immobilized via 1-ethyl-3-(3-dimethylaminopropyl) carbodiimide hydrochloride (EDC)/*N*-hydroxysuccinimide (NHS) chemistry onto $\text{Fe}_3\text{O}_4@Ag@MPA$ nanoparticles for the first time to remove phenolic compounds and dyes from aqueous media. Characterization of nanoparticles was performed by Fourier-transform infrared spectroscopy (FTIR), transmission electron microscopy (TEM) and energy dispersive X-ray (EDX) analysis and electron spin resonance (ESR) techniques. Kinetic properties of free and immobilized tyrosinases were studied using L-catechol and L-tyrosine as substrates. Thermal, storage and operational stabilities of free and immobilized tyrosinase were determined. The performance of immobilized tyrosinase on decolorization of selected azo dyes and phenolic compounds was evaluated. Additionally, electrochemical catechol sensing ability of immobilized tyrosinase was investigated by CV.

2 Materials and Methods

2.1 Materials

Tyrosinase (EC 1.14.18.1) from mushroom (T3824, 25 KU), Bradford reagent, NH_4OH solution (24%), AgNO_3 , NaBH_4 , 1-ethyl-3-(3-dimethylaminopropyl) carbodiimide hydrochloride (EDC), *N*-hydroxysuccinimide (NHS), L-catechol, Bisphenol A, Nafion, 4-aminoantipyrene (4-AAP) and azo dyes were obtained from Sigma-Aldrich (St. Louis, USA). $\text{FeCl}_3 \cdot 6\text{H}_2\text{O}$, $\text{FeCl}_2 \cdot 4\text{H}_2\text{O}$, $\text{K}_3\text{Fe}(\text{CN})_6$, NaHCO_3 and ethanol were supplied from Merck (Darmstadt, Germany). 3-Mercaptopropionic acid (MPA), L-tyrosine, phenol, Bisphenol F, Bisphenol B, *p*-cresol, 1-naphthol, 4-tertiary butylphenol and phenyl acetate were supplied from Alfa Aesar (Kandel, Germany). *p*-Aminophenol, 3-chlorophenol and 4-chlorophenol were purchased from CDH Chemicals, India. Ultra-pure

water (18.2 M Ω cm) obtained from Millipore Simplicity® (France) water purification system was used to prepare all the solutions throughout this study. A double-beam spectrophotometer (Shimadzu UV-1601, Japan) was used for optical measurements. Metrohm DropSens-DRP-110 (Spain, Llanera) screen-printed carbon electrodes (SPCE) were used for electrochemical measurements.

2.2 Fabrication of 3-Mercaptopropionic Acid-Attached Silver-Coated Magnetite (Fe₃O₄@Ag@MPA) Nanoparticles

Synthesis of Fe₃O₄@Ag@MPA nanoparticles was carried out according to previous studies [22, 23]. Bare magnetic nanoparticles (Fe₃O₄) were produced via chemical co-precipitation of Fe³⁺ and Fe²⁺ ions. Briefly, 1.04 g of FeCl₃·6H₂O and 0.386 g of FeCl₂·4H₂O were separately dissolved in 100 mL aliquots of deionized water. The solutions were mixed and 20 mL of ammonia solution (24%) was added. The solution was mixed at 400 rpm for 1 h at room temperature. Finally, magnetic nanoparticles were separated using an external magnet and washed with deionized water for three times. Silver coating of the as-prepared bare nanoparticles was carried out by dispersing them in 100 mL of deionized water, mixing with AgNO₃ solution (0.086 g/100 mL) and 10 mg of NaBH₄ (Fig. S1). Silver-coated magnetic nanoparticles (Fe₃O₄@Ag) were separated with a magnet and washed three times with deionized water. For the attachment of MPA onto Fe₃O₄@Ag, 100 mL of 0.01 M ethanolic MPA solution was added onto Fe₃O₄@Ag and stirred at 400 rpm for 24 h at 25 °C. Finally, prepared nanoparticles were separated with an external magnet and washed three times with deionized water and dispersed in 100 mL of 0.1 M pH 5.5 phosphate buffer (PBS) solution.

2.3 Tyrosinase Immobilization Onto Fe₃O₄@Ag@MPA Nanoparticles

Tyrosinase was covalently immobilized onto Fe₃O₄@Ag@MPA nanoparticles via EDC/NHS coupling [24]. For this, Fe₃O₄@Ag@MPA nanoparticles from 5.0 mL of dispersion (containing 8.5 mg nanoparticle) in 0.1 M pH 5.5 phosphate buffer was mixed with 0.39 g of EDC and 0.058 g of NHS to obtain a final concentration of 400 mM and 100 mM EDC and NHS, respectively. After stirring for 30 min, to obtain 2.0 mg/mL final concentration, calculated amount of tyrosinase was added. Coupling reaction proceeded for 24 h at +4 °C with gentle stirring (Fig S1). Protein contents of the initial and final nanoparticle dispersions were determined using Coomassie Brilliant Blue reagent, following the Bradford's method using bovine serum albumin as standard [25]. The amount of immobilized TYR was calculated from Eq. 1:

$$Q = (C_0 - C)V/m \quad (1)$$

where, Q is the amount of immobilized TYR on a unit mass of the nanoparticles (mg/g); C_0 and C are the TYR concentrations in the initial and final solutions, respectively (mg/mL); V is the volume of the solution (mL); and m is the mass of the nanoparticles. Additionally, immobilization yield (IY) and immobilization efficiency (IE) was calculated by the following formulas:

$$IY = [(m_0 - m)/m_0] \times 100 \quad (2)$$

$$IE = (a_i/a_f) \times 100 \quad (3)$$

where, m_0 is the initial amount of tyrosinase before immobilization, m is the tyrosinase amount remained in the solution after immobilization, a_i and a_f are the total activities of immobilized enzyme and free enzyme, respectively.

2.4 Characterization of Fe₃O₄@Ag@MPA Nanoparticles

Characterization of dried Fe₃O₄@Ag@MPA nanoparticles was conducted by FTIR, TEM-EDX, and ESR techniques. Morphological and structural properties of nanoparticles were evaluated by TEM images and EDX analysis which were examined by a Jeol JEM2100 transmission electron microscope. FTIR spectra were recorded using an FTIR spectrophotometer (Perkin Elmer Spectrum 100, UK) on ATR mode. ESR spectrum was obtained from JEOL-JESFA 300 ESR spectrometer to demonstrate the magnetic character of synthesized nanoparticles.

2.5 Activity Measurements of Free and Immobilized Tyrosinase

Two substrates, L-catechol and L-tyrosine, were used in order to compare the activity of tyrosinase against different substrates. For free tyrosinase, reaction was carried out with 1.40 mL of 2.0 mM L-catechol (in 0.1 M PBS, pH 7.0) and 0.1 mL of 0.1 mg/mL tyrosinase solution for 2 min [26], whereas 1.45 mL of 1.0 mM L-tyrosine (in pH 6.5 0.1 M PBS) was reacted with 0.05 mL of 1.0 mg/mL of TYR solution for 10 min [13]. One unit of enzyme activity was defined as the amount of enzyme that produces one micromole of *o*-quinone ($\epsilon_{420} = 3450 \text{ M}^{-1} \text{ cm}^{-1}$) per minute at 420 nm and 25 °C with L-catechol. Additionally, one unit was defined as the increase in A_{280} of 0.001 per minute at pH 6.5 at 25 °C in a reaction mixture containing L-tyrosine. Activity measurements of immobilized tyrosinase was carried out using nanoparticles from 1.0 mL of nanoparticle dispersion obtained by magnetic separation. Substrate solutions (1.5 mL) were added onto magnetically-precipitated

nanoparticles and incubated for 2 min for L-catechol and 10 min for L-tyrosine at 25 °C. Magnetic nanoparticles were precipitated with a magnet and the absorbance of the supernatants were measured. Free and immobilized TYR activities were determined at different pHs with 0.1 M buffer solutions (pH 4.0–5.0 acetate, pH 6.0–8.0 phosphate and pH 9.0 carbonate) and various temperatures between 4 and 65 °C.

2.6 Determination of the Kinetic Constants

Kinetic parameters, K_m and V_{max} , were determined by measuring the catalytic activities of free and immobilized tyrosinase at different concentrations of L-tyrosine (0.10–2.00 mM) and L-catechol (0.30–10.0 mM) at optimum pH and temperature for each substrate. The data calculated using Lineweaver–Burk equation (Eq. 4) were plotted and K_m and V_{max} were estimated from the intercepts at x - and y -axis of the plot, respectively.

$$1/v = [K_m/V_{max}[S]] + 1/V_{max} \quad (4)$$

2.7 Determination of Thermal, Operational and Storage Stability

The thermal stability experiments were performed by treating free tyrosinase solution and tyrosinase-immobilized nanoparticles at 45 °C in 0.1 M pH 7.0 PBS in a thermostated water bath (Daihan Wisebath WB-22, Korea). Samples were withdrawn at defined time intervals and subjected to activity measurement immediately.

Operational stability of immobilized tyrosinase was examined by performing consecutive activity measurements with the same TYR-bound nanoparticles using 2.0 mM L-catechol at 25 °C. Activity measurements were repeated with a fresh aliquot of substrate after the immobilized tyrosinase was separated magnetically and washed with 1.0 mL of 0.1 M pH 7.0 PBS buffer.

Storage stabilities of the free and immobilized tyrosinases were determined by storing the relevant enzymes in 0.1 M pH 6.5 PBS at 4 °C. Residual activities of free and immobilized tyrosinases were measured at various days. Initial activity of each sample was regarded as 100% and relative activities were calculated.

2.8 Dye Decolorization with Immobilized Tyrosinase

Decolorization of selected mono azo dyes [SYF: Sunset Yellow FCF (λ_{max} : 481 nm) and PR: Procion Red MX5B (λ_{max} : 536 nm)] and diazo dyes [CR: Congo Red (λ_{max} : 484 nm) and RG: Reactive Green 19 (λ_{max} : 627 nm)] by

immobilized tyrosinase was determined by monitoring the decrease in absorbance at their maximum wavelengths. Experiments were performed with 10 mg/L dye solutions prepared by dissolving each dye in 0.1 M pH 6.5 PBS and pH 4.0 acetate buffers at 30 °C. Tyrosinase immobilized nanoparticles (precipitated from 1.5 mL of nanoparticle dispersion) were interacted with 10.0 mL of dye solutions and UV–vis spectra were recorded at different time intervals during the enzymatic treatment after the reaction medium was centrifuged at $18,000\times g$ at +4 °C for 10 min. Decolorization percent was calculated by the equation below:

$$\text{Decolorization (\%)} = \frac{(A_i - A_f)}{A_i} \times 100 \quad (5)$$

where, A_i was the initial absorbance and A_f was the final absorbance of dye solution.

2.9 Removal of Phenolic Compounds with Immobilized Tyrosinase

Immobilized tyrosinase was investigated for its phenolic removal ability using phenol, Bisphenol F, Bisphenol A, Bisphenol B, *p*-cresol, phenyl acetate, 3-chlorophenol, 4-chlorophenol, *p*-aminophenol, 4-*tert*-butylphenol, and 1-naphthol as model compounds. For this purpose, 5.0 mL of oxygen-saturated 0.2 mM phenolic compound solution (in 0.01 M PBS pH 7.0) was mixed with 500 μ L dispersion of Fe₃O₄@Ag@MPA-TYR nanoparticles (0.8 mg nanoparticles). The reaction mixture was shaken using a benchtop shaker (Promax 2020, Heidolph Instruments GmbH & Co KG, Kelheim, Germany) at 50 rpm at 25 °C for 24 h. The initial and final phenolic compound concentrations were determined by applying 4-aminoantipyrine spectrophotometric method in which the residual phenolic compound reacts with the primary amine of 4-AAP and results an intermediate which is oxidized by potassium ferricyanide yielding a red quinone-type dye that absorbs at 510 nm [6]. For this assay, 0.1 mL of 4-AAP solution (20 mM in 0.25 M NaHCO₃) and 0.1 mL of potassium ferricyanide solution (83.4 mM in 0.25 M NaHCO₃) were mixed with 0.8 mL of aqueous phenolic sample. After 10 min, absorbance of the solutions was measured by UV–Vis spectrophotometer at 510 nm. All solutions were prepared freshly. Phenol removal ratio was calculated from the equation below:

$$\text{Phenol removal ratio(\%)} = \frac{(P_i - P_r)}{P_i} \times 100 \quad (6)$$

where P_i and P_f are the initial and the final phenol concentrations of the solutions, respectively.

2.10 Electrochemical Behavior of Tyrosinase Immobilized $\text{Fe}_3\text{O}_4@Ag@MPA$ Nanoparticles

In order to evaluate the availability of tyrosinase immobilized $\text{Fe}_3\text{O}_4@Ag@MPA$ nanoparticles ($\text{Fe}_3\text{O}_4@Ag@MPA\text{-TYR}$) for biosensor studies, the electrochemical sensing behavior was determined in presence of L-catechol. For this, 5.0 μL of free tyrosinase solution and immobilized tyrosinase dispersion were drop-casted onto screen-printed carbon electrode (SPCE) surface. Outermost surfaces of the working electrodes were covered by 5.0 μL 1.0% Nafion solution. All solutions were prepared with pH 0.1 M 6.0 PBS with 0.1 M KCl. Cyclic voltammetry (CV) was applied to obtain the electrochemical response of immobilized tyrosinase towards L-catechol (100 μL , 1.0 mM) at a scan rate of 100 mV/s in the potential range of -500 mV to $+800$ mV using PalmSens4 potentiostat (The Netherlands). The voltammogram of bare electrode was also recorded.

3 Results and Discussion

3.1 Characterization of Bare and $\text{Fe}_3\text{O}_4@Ag@3\text{-Mercaptopropionic Acid-Tyrosinase Nanoparticles}$

Magnetic nanoparticles are extensively used and attractive materials for several applications including medicine, biotechnology, drug delivery, bioseparations and biomolecule immobilization [22]. Their promising properties such as easy separation from the medium by an external magnetic field, modification with several functional groups, and large surface area make them fascinating materials [6]. Herein, $\text{Fe}_3\text{O}_4@Ag@3\text{-mercaptopropionic acid}$ nanoparticles were fabricated for tyrosinase immobilization and characterization of the nanoparticles was carried out by FTIR, TEM and EDX analysis, and ESR techniques.

FTIR spectra confirmed that $\text{Fe}_3\text{O}_4@Ag$ nanoparticles were modified with MPA. The C=O stretching and $-\text{CH}_2$ deformation of MPA resulted in the spectrum of Ag-MPA at $1600\text{--}1400\text{ cm}^{-1}$. Additionally, the S-H stretching of MPA at 2568 cm^{-1} disappeared revealing that MPA was bound through $-\text{SH}$ groups to Ag bearing Fe_3O_4 nanoparticles. Modification of Fe_3O_4 nanoparticles with Ag and MPA, respectively, was proved as shown in Fig. S2 and the results were consistent with previous results [27, 28].

TEM micrograph of $\text{Fe}_3\text{O}_4@Ag@MPA$ nanoparticles is shown in Fig. 1a. Nanoparticles were almost spherical and uniform. The light shell around the dark core of Fe_3O_4 corresponds to coating with Ag and functionalization with

MPA. Incorporation of Ag and MPA and immobilization of tyrosinase onto nanoparticles was also proved by TEM-EDX mapping (Fig. 1b-d). As seen from EDX spectrum (Fig. S3), Ag and S elements come from coating magnetite nanoparticles with Ag and further functionalizing with MPA, respectively. Appearance of Cu element resulted from the immobilization of tyrosinase onto the nanoparticles since tyrosinase is a copper-bearing enzyme. It was calculated that 216.6 ± 1.250 mg TYR was immobilized onto one gram of $\text{Fe}_3\text{O}_4@Ag@MPA$ nanoparticles with an immobilization yield of 33.7%. Immobilization efficiency was calculated to be 48.7% with L-catechol and 28.6% with L-tyrosine.

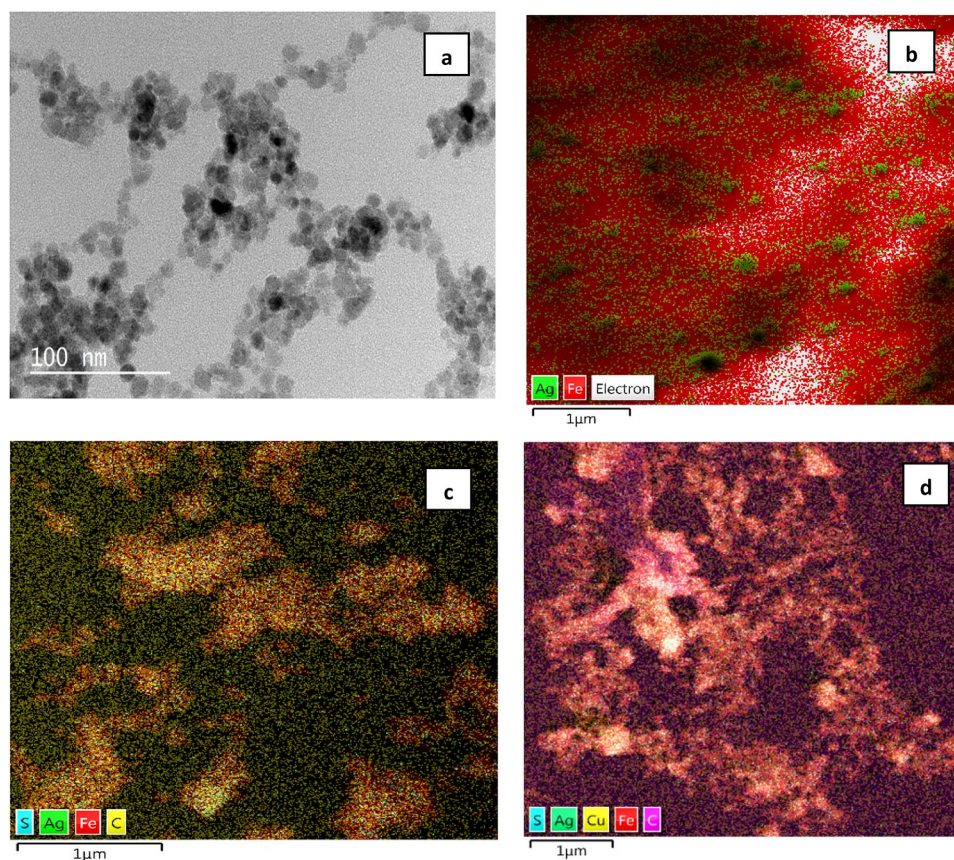
Magnetic property of $\text{Fe}_3\text{O}_4@Ag@MPA$ nanoparticles was confirmed by ESR analysis. The g factor was calculated using $g = hv/\beta H_r$ equation; where, h is Planck's constant (6.626×10^{-27} erg/s); ν is the frequency (9.707×10^9 Hz); β is the universal constant (9.274×10^{-21} erg/G), and H_r is the resonance of magnetic field (G). Magnetic character of synthesized nanoparticles was evidenced as seen in Fig. S4, since the g factor was 2.3 which was convenient with the g factor of Fe^{3+} (1.4–3.0 for low-spin complex and 2.0–9.7 for high spin complex) [22, 29].

3.2 Activities of Free and Immobilized Tyrosinase

Changes in acidic or basic conditions of the media in which enzymatic reactions take place affect enzyme activity since amino acid residues around the active site may be subjected to structural or conformational changes. When it comes to immobilized enzymes, new interactions are involved that occur between functional groups of the support material and the enzyme molecule [30]. Here, activity measurements of free and immobilized tyrosinase were performed at pH 4.0–9.0 using L-catechol and L-tyrosine. pH-activity profiles of free and immobilized tyrosinase were depicted in Fig. 2a and b. Optimum pH was 7.0 with L-catechol whereas it was pH 6.5 with L-tyrosine for both forms of tyrosinase. These results were consistent with the studies of Dinçer et al. [31] and Aytar and Bakir [32]. With L-tyrosine, free enzyme showed activity in a wider range compared to immobilized one, however, this difference may result from covalent immobilization. A similar narrow pH-activity profile was obtained by Çakmak et al. [33] where lipase was covalently bound onto epichlorohydrin coated magnetic nanoparticles.

The effect of reaction medium temperature on relative activities of free and immobilized tyrosinase was examined by performing the enzymatic reaction at different temperatures between 4 and 65 °C. Relative activities of free and immobilized TYR as a function of temperature were compared in Fig. 3a, b. Optimum temperature of free tyrosinase was 45 °C whereas it was 35 °C for immobilized TYR when L-catechol was used as substrate. It may be considered that the conformational flexibility of tyrosinase was altered to

Fig. 1 Visual characterization of magnetic nanoparticles. Transmission electron microscopy (TEM) image (a) and transmission electron microscopy-energy dispersive X-ray (TEM-EDX) mapping of $\text{Fe}_3\text{O}_4@Ag$ (b), $\text{Fe}_3\text{O}_4@Ag@MPA$ (c) and tyrosinase immobilized $\text{Fe}_3\text{O}_4@Ag@MPA$ (d) nanoparticles



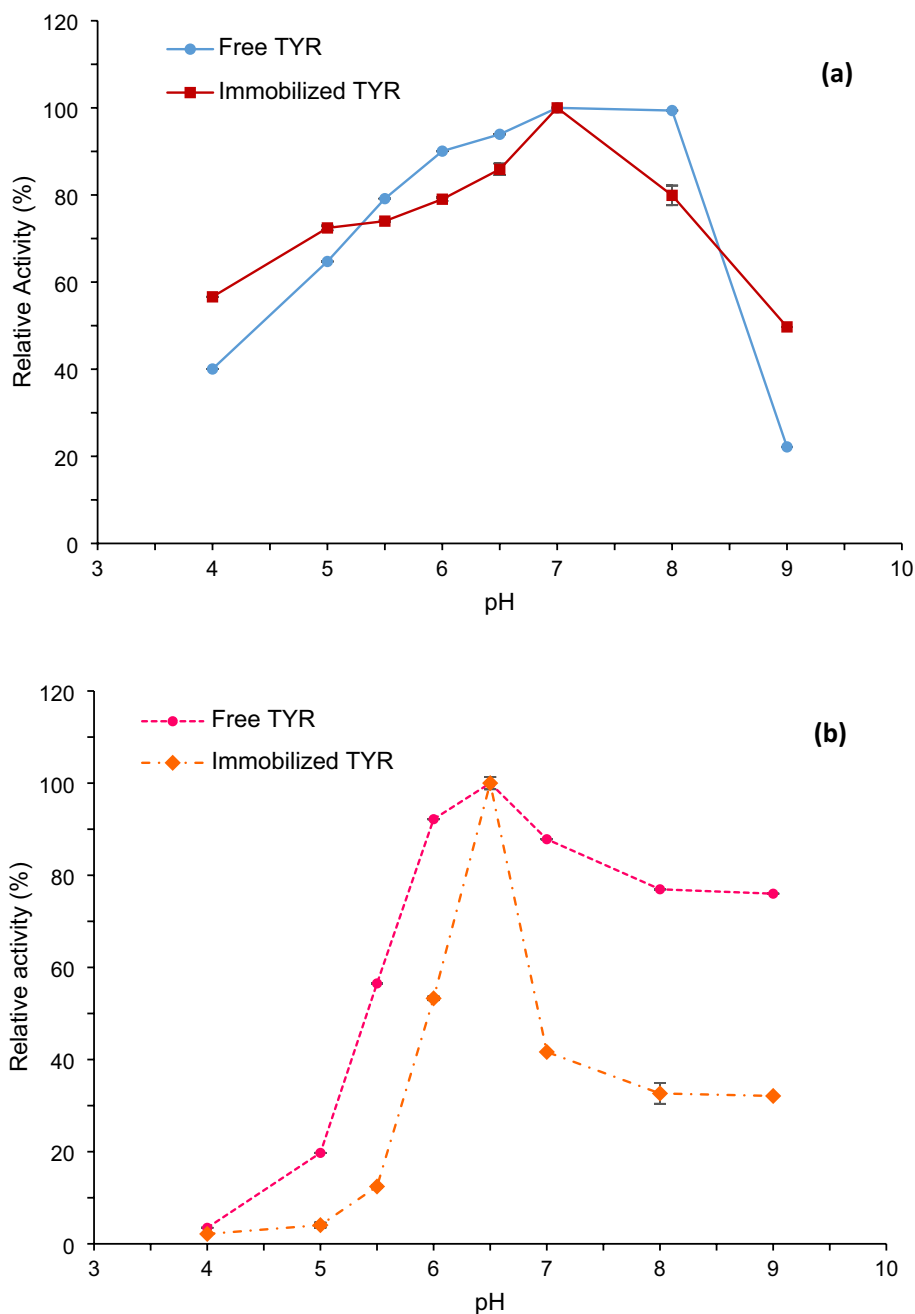
bind *L*-catechol substrate easier and required lower activation energy for catalysis than free TYR after immobilization. Both free and immobilized TYR reached its maximum activity at 45 °C when the substrate was *L*-tyrosine. Immobilized form of tyrosinase exhibited broader temperature-activity profile with both of the substrates indicating a better heat-resistance compared to the free form in accordance with the work of Liu et al. [9] and Arıca et al. [34]. Enzyme activity decreased above the optimum temperatures of free and immobilized tyrosinases since denaturation occurs. Additionally, aggregation of tyrosinase immobilized nanoparticles was observed resulting decrease in enzymatic activity at temperatures above 45 °C.

3.3 Kinetic Parameters

The kinetic constants, K_m and V_{max} of free and immobilized tyrosinase were calculated from Lineweaver–Burk plots, by measuring the initial reaction rates at different substrate concentrations at optimum pH and optimum temperature. *L*-catechol (0.30–10.0 mM) and *L*-tyrosine (0.10–2.00 mM) was used for kinetic studies. As depicted in Table 1, K_m of immobilized tyrosinase was lower than the K_m of free tyrosinase with both *L*-catechol and

L-tyrosine. The lower K_m value for immobilized enzyme revealed that immobilization provided a stabilization effect that increased the affinity of the enzyme towards its substrates. A similar result was reported by Liu et al. where tyrosinase was immobilized on $\text{Fe}_3\text{O}_4\text{-NH}_2$ nanoparticles by a combination of physical adsorption and covalent crosslinking and K_m for free and immobilized tyrosinase were calculated to be 1.00 and 0.36 mM, respectively [9]. However, contrary results may be encountered that K_m of tyrosinase increases upon immobilization due to diffusional limitations and steric hindrances [14, 31]. V_{max} of tyrosinase decreased after immobilization by 2-fold and 3.8-fold related to *L*-catechol and *L*-tyrosine substrates, respectively, in comparison to free enzyme. It can be assumed that upon immobilization, the conversion rates of substrates into products could be slower due to diffusional limitations or steric effects caused by the strict conformation of the bound enzyme. However, herein, immobilized tyrosinase can provide activity with a low decline similar to the results reported by Wu et al. where tyrosinase was covalently immobilized on polyacrylonitrile beads and V_{max} of free tyrosinase (22.73 U/mg protein) was higher than V_{max} of immobilized enzyme (18.61 U/mg protein) [35].

Fig. 2 Effect of medium pH on the activities of free and immobilized tyrosinase **a** with L-catechol and **b** with L-tyrosine



3.4 Thermal, Operational and Storage Stabilities of Free and Immobilized Tyrosinase

Thermal stabilities of free and immobilized tyrosinase were determined by measuring the activities of the enzymes after incubating the enzymes in absence of substrate at 45 °C for 150 min. As seen from Fig. 4a, free TYR was inactivated at a higher rate than the immobilized form. Immobilized TYR conserved 42% of its initial activity, whereas free TYR conserved only 11% in 15 min. Additionally, free enzyme was totally inactive after 60 min of incubation.

Storage of enzymes in their soluble forms generally cause decline in their activities due to the loss of stability. Immobilization is a useful route to preserve enzyme activity during storage to provide a longer shelf-life. Covalent immobilization helps the enzyme molecules to be kept safe from the distortions caused by the aqueous environment compared to its free counterpart [35]. As illustrated in Fig. 4b, after 84 days of storage at 4 °C, residual activities of free and immobilized TYR were $45.9 \pm 2.4\%$ and $68.4 \pm 2.6\%$, respectively. In accord with the results of Liu et al., immobilized TYR indicated higher stability than free TYR due to the stabilization through the covalent attachment of the enzyme [9].

Fig. 3 Effect of temperature on the activities of free and immobilized tyrosinase **a** with L-catechol and **b** with L-tyrosine

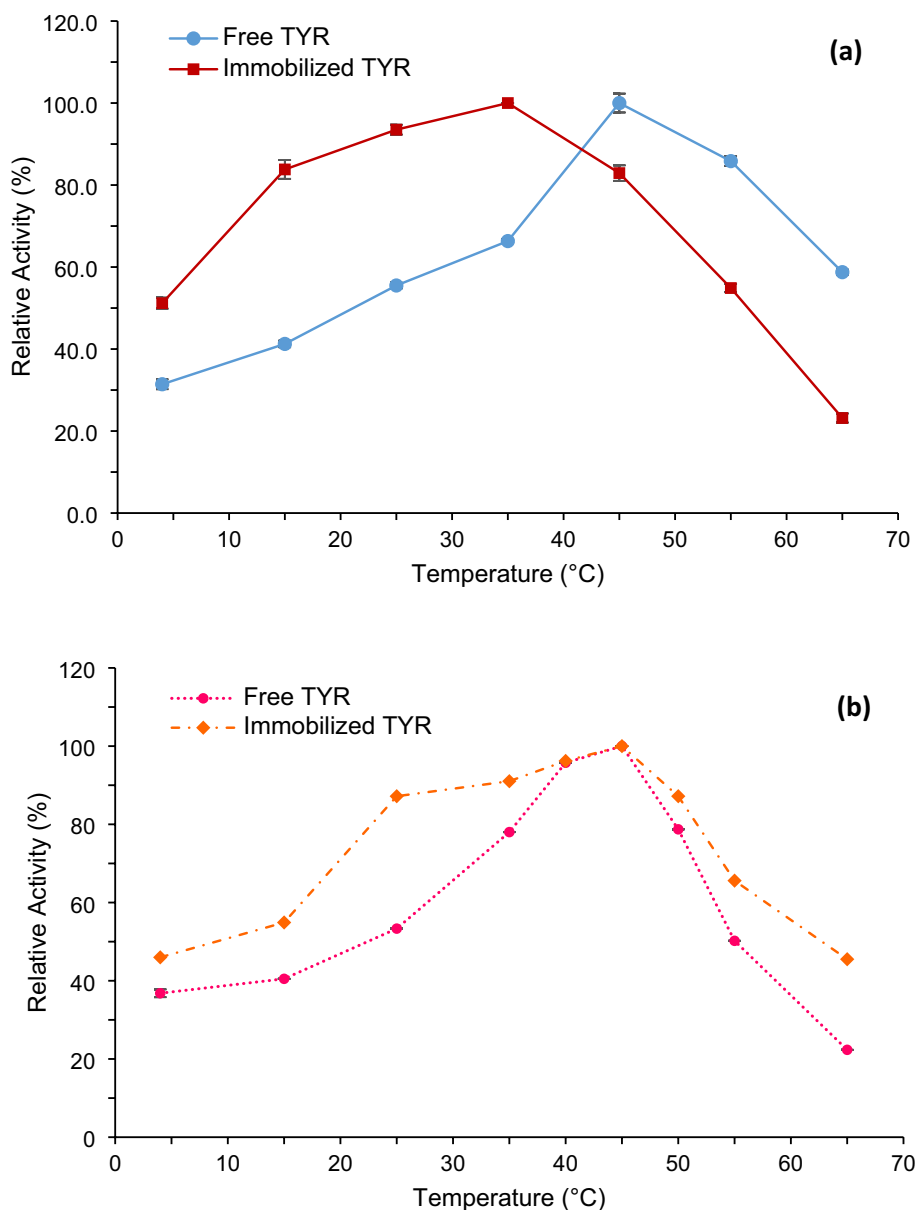


Table 1 Kinetic constants of free and immobilized tyrosinase. K_m and V_{max} values measured with L-catechol and L-tyrosine substrates

Kinetic parameter	Free tyrosinase		Immobilized tyrosinase	
	L-catechol	L-tyrosine	L-catechol	L-tyrosine
K_m (mM)	0.62	0.571	0.439	0.428
V_{max} ($\mu\text{mol}/\text{min}$)	0.666	178.6	0.302	46.7

The knowledge of operational stability of an immobilized enzyme is an important parameter to evaluate the industrial exploitation of the carrier-bound biocatalyst [36]. In order to investigate the reusability of immobilized TYR, several repetitive activity measurements of immobilized TYR with

L-catechol were operated. Nanoparticles were separated magnetically after each measurement and washed with 0.1 M pH 7.0 PBS and got ready for the next run. Figure 4c depicts that immobilized TYR gradually lost its activity until the 10th cycle. It was able to oxidize L-catechol by 50% at the 6th cycle. The reusability of covalently-immobilized TYR onto $\text{Fe}_3\text{O}_4\text{-NH}_2$ nanoparticles was evaluated by Liu et al. and 61.4% residual activity was reported after five reuses [9].

3.5 Dye Decolorization and Phenolic Compound Removal with Immobilized Tyrosinase

Azo dyes are widely used in textile, paper, food, cosmetics and leather industries. However, discharge of effluents

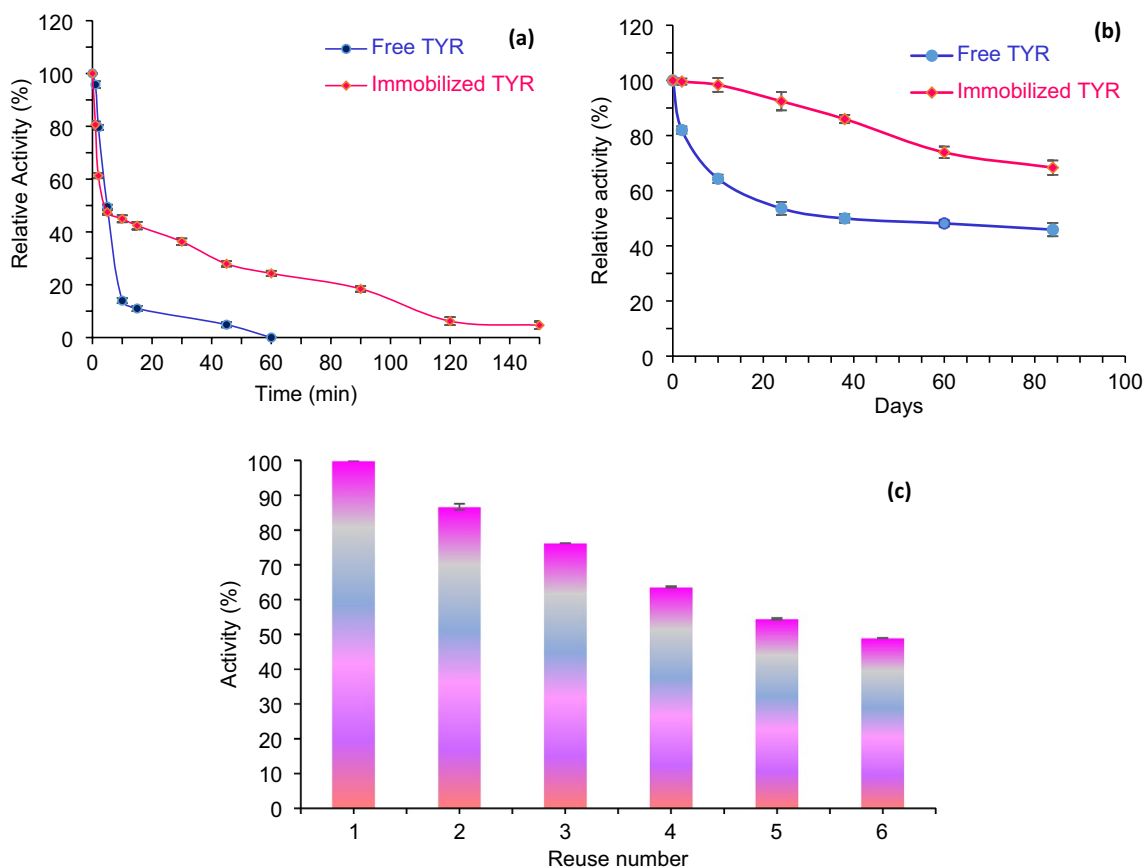


Fig. 4 Stability profiles of tyrosinase preparations. **a** Thermal (45 °C), **b** storage stabilities (+4 °C) of free and immobilized tyrosinase, **c** operational stability of immobilized tyrosinase

Table 2 Decolorization efficiency of immobilized tyrosinase

Dye (10 mg/L)	pH	SYF	RG	CR	PR
Decolorization (%)	4.0	13.6 ± 1.23	36.9 ± 2.34	95.0 ± 0.65	22.2 ± 0.87
	6.5	4.87 ± 1.15	13.5 ± 0.35	21.5 ± 1.32	9.28 ± 0.49

containing azo dyes, especially synthetic ones, may cause serious environmental problems since they are recalcitrant and persistent [3]. Enzymatic treatment of dyes gained considerable attention in order to provide more efficient, cheaper and greener approach as an alternative to conventional chemical or physical treatment procedures [37]. Oxidoreductases such as laccases, peroxidases and tyrosinases have been used for dye removal or decolorization [4]. The potential of tyrosinase enzyme immobilized on Fe₃O₄@Ag@MPA nanoparticles to decolorize selected azo dyes was evaluated.

Decolorization percents of 10 mg/L SYF, RG, CR and PR by immobilized tyrosinase at 30 °C at pH 4.0 and 6.5 were determined. Decolorization percent of Congo Red reached 95.0 ± 0.65, whereas it was lower for other azo dyes used in this study. Congo Red was similarly decolorized with a high percent in the work of Suryamathi et al. where 94% of methyl orange and Congo Red azo dyes were decolorized with tyrosinase immobilized on electrospun zein nanofibrous matrix [19]. As indicated in Table 2, decolorization was higher at pH 4.0 than pH 6.5. Although the optimum pH of immobilized tyrosinase was 6.5, decolorization was better at acidic pH. In accordance with the results of Arabaci and Usluoğlu, decolorization percent was higher at pH 4.0 than at pH 7.0, and that phenomenon can provide an advantage for decolorization of acidic effluents [21]. Figure S5 depicts the absorbance spectra of dye solutions before and after 24 h of treatment with immobilized tyrosinase at pH 4.0.

Optimum pH may vary with different substrates as well as interactions between dyes and immobilized TYR may be favorable at acidic pH. Temperature was held constant at 30 °C for decolorization experiments and optimum reaction period was 24 h. Decolorization of dye solutions decreased at longer reaction periods more than 24 h which may be attributed to enzyme inactivation. Longer interaction between enzyme and substrate may increase enzymatic conversion but sometimes inactivation may occur as stated by da Silva et al. [37] where degradation of Reactive Blue 114 dye decreased after 24 h of reaction.

Tyrosinase is a well-known enzyme with its efficiency to remove several phenolic compounds present in wastewaters [17]. Removal efficiencies of tyrosinases covalently immobilized on various support materials towards some phenolic compounds were reported in literature. Polyacrylonitrile beads modified with glutaraldehyde were prepared as immobilization supports for tyrosinase immobilization and used for degradation of phenol resulting 96% removal efficiency [35]. Bisphenol A, Bisphenol B and Bisphenol F were degraded by immobilized tyrosinase on polyacrylonitrile beads with removal efficiencies of 92, 93 and 94%, respectively [36]. Bisphenol derivatives such as Bisphenol A, Bisphenol B, Bisphenol C, Bisphenol F, Bisphenol S are widely used in epoxy resin and polycarbonate plastic manufacturing [38]. These compounds vary with the groups present between two phenol groups. In this study, phenol, Bisphenol F, *p*-cresol, phenyl acetate, Bisphenol A, 3-chlorophenol and 4-chlorophenol were removed from aqueous solutions by ratios of $82.5 \pm 1.25\%$, $65.0 \pm 2.41\%$, $73.1 \pm 1.85\%$, $92.3 \pm 2.12\%$, $39.3 \pm 1.32\%$, $50.5 \pm 1.54\%$ and $87.8 \pm 1.64\%$, respectively, in 24 h by immobilized tyrosinase onto $\text{Fe}_3\text{O}_4@Ag@MPA$ nanoparticles (Table 3). However, no removal was detected in case of *p*-aminophenol, 4-*tert*-butylphenol, Bisphenol B and 1-naphthol. Yamada et al. [39] reported that 4-*tert*-butylphenol oxidation by mushroom tyrosinase could be achieved in presence of hydrogen peroxide, therefore it can be understandable that no conversion was determined with that phenolic compound in our study. Although tyrosinase was reported to have no action on BPA in absence of H_2O_2 [40], as stated by Suzuki et al. [38], BPA was slowly converted into quinone derivatives without H_2O_2 present; similar to our results. The high removal of *p*-cresol and 4-chlorophenol was attributed to the electron-donating substituents at para position [41]. High removal efficiencies were also reported for *p*-cresol by diatom biosilica-immobilized tyrosinase (74%) [42] and for *p*-chlorophenol by cross-linked tyrosinase aggregates (100%) [41]. The removal efficiency of immobilized

tyrosinase is supposed to be both dependent on the phenolic compound molecular structure and the nature of the immobilized enzyme system.

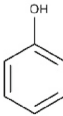
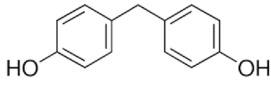
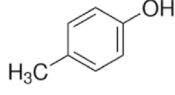
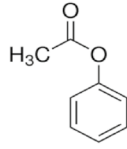
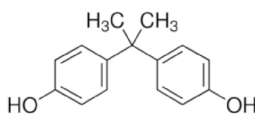
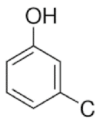
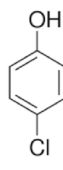
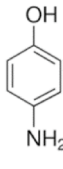
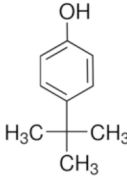
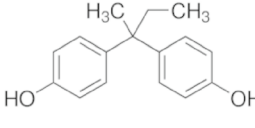
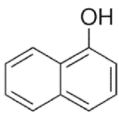
3.6 Electrochemical Studies of Tyrosinase- $\text{Fe}_3\text{O}_4@Ag@MPA$ Nanoparticles

Cyclic voltammetry (CV) is an electrochemical technique which is used to evaluate the modifications on the electrode surface. In this presented work, electrode surface was modified with TYR immobilized silver coated magnetic nanoparticles. CV measurements were carried out in presence of 1.0 mM catechol within the potential range of -500 to $+800$ mV. Catechol demonstrated two peaks (anodic and cathodic) due to its transformation to *o*-quinone. The CV results of the presented study are shown in Fig. 5. As clearly seen here, electrochemical response of catechol was significantly increased by the incorporation of $\text{Fe}_3\text{O}_4@Ag@MPA$ nanoparticles similar to the study of Erkmen et al. [43] where tyrosinase was immobilized on poly(3,4-ethylenedioxythiophene) iridium oxide nanocomposite for detection of catechol and azinphos methyl.

4 Conclusion

Water pollution caused by dyes and phenolic compounds has been a world-wide problem. Therefore, it is essential to develop new efficient methods as alternatives to conventional ones for water remediation. Enzymes capable of degrading dyes and phenolics are good candidates for that purpose. As a promising biocatalyst for treatment of wastewaters, tyrosinase has been employed for removal of pollutants in several studies both in its free and immobilized forms. In presented work, a novel candidate to augment the traditional wastewater treatment for removal of phenolic compounds and azo dyes was developed by modifying Fe_3O_4 with Ag and MPA for covalent immobilization of TYR via EDC/NHS chemistry. The affinity of tyrosinase towards the substrates was improved as well as storage, operational and thermal stabilities in comparison to free enzyme after immobilization. The results proved that immobilized TYR appeared as an efficient nanobiocatalyst incorporating the advantages such as easy use and separation, stability and reusability with remarkable efficiency of decolorization and dephenolization. Additionally, a promising nanoparticulate support material was developed that can be expanded for immobilization of other enzymes as well as for further biosensor applications.

Table 3 Dephenolization potential of immobilized tyrosinase

Phenolic compound (0.2 mM)	Molecular structure	Dephenolization (%)
Phenol		82.5±1.25
Bisphenol F		65.0±2.41
<i>p</i> -cresol		73.1±1.85
Phenyl acetate		92.3±2.12
Bisphenol A		39.3±1.32
3-chlorophenol		50.5±1.54
4-chlorophenol		87.8±1.64
<i>p</i> -aminophenol		—
4- <i>tert</i> -Butylphenol		—
Bisphenol B		—
1-naphthol		—

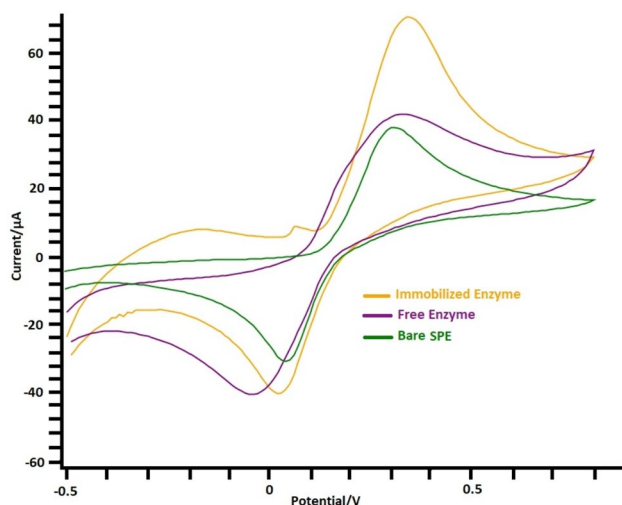


Fig. 5 Cyclic voltammetry characterization of free and immobilized tyrosinase behavior

Supplementary Information The online version contains supplementary material available at <https://doi.org/10.1007/s10562-022-04087-z>.

Acknowledgements The authors are grateful to the Aydın Adnan Menderes University Scientific Research Fund for financially supporting this research under Project Number FEF 20012.

Author Contributions RY: Visualization, Validation, Investigation, Writing-original draft preparation. DAU: Conceptualization, Methodology, Writing-reviewing-editing. AAK: Supervision, Conceptualization, Writing-reviewing-editing.

Declarations




Conflict of interest The authors declare that they have no known competing financial interests or personal relationships that could have appeared to influence the work reported in this paper.

References

- Li T, Song HL, Xu H et al (2021) *J Hazard Mater* 416:125864
- Sellami K, Couvert A, Nasrallah N et al (2021) *J Hazard Mater* 403:124021
- Veismoradi A, Mousavi SM, Taherian M (2019) *J Chem Technol Biotechnol* 94:3559–3568
- Jun LY, Yon LS, Mubarak NM et al (2019) *J Environ Chem Eng* 7:102961
- Lu Y, Yan L, Wang Y et al (2009) *J Hazard Mater* 165:1091–1097
- Abdollahi K, Yazdani F, Panahi R et al (2018) *3 Biotech* 8:1–10
- Liang S, Wu X, Xiong J et al (2020) *Coord Chem Rev* 406:213149
- Mulinari J, Oliveira V, Hotza D (2020) *Biotechnol Adv* 42:107581
- Liu DM, Chen J, Shi YP (2018) *Anal Chim Acta* 1006:90–98
- Bilal M, Rasheed T, Zhao Y et al (2018) *Int J Biol Macromol* 119:278–290
- Sharifi M, Karim AY, Nanakali NMQ et al (2020) *J Biomol Struct Dyn* 38:2746–2762
- Nelson JM, Griffin EG (1916) *J Am Chem Soc* 38:1109–1115
- Peniche H, Osorio A, Acosta N et al (2005) *J Appl Polym Sci* 98:651–657
- Abdollahi K, Yazdani F, Panahi R (2019) *J Biol Inorg Chem* 24:943–959
- Liu Z, Deng J, Li D (2000) *Anal Chim Acta* 407:87–96
- Faccio G, Kruus K, Saloheimo M et al (2012) *Process Biochem* 47:1749–1760
- Min K, Park GW, Yoo YJ et al (2019) *Bioresour Technol* 289:121730
- Espín JC, Varón R, Fenoll LG et al (2000) *Eur J Biochem* 267:1270–1279
- Suryamathi M, Viswanathamurthi P, Vennila K et al (2021) *Fibers Polym* 22:2714–2725
- Wu FC, Tseng RL, Juang RS (2001) *J Hazard Mater* 81:167–177
- Arabaci G, Usluoglu A (2014). *Sci World J*. <https://doi.org/10.1155/2014/685975>
- Akduman B, Uygun M, Uygun DA et al (2013) *J Nanopart Res* 15:1564
- Marques FC, Oliveira GP, Teixeira RA et al (2018) *Vib Spectrosc* 98:139–144
- Uygun M, Jurado-Sanchez B, Uygun DA et al (2017) *Nanoscale* 9:18423–18429
- Bradford MM (1976) *Anal Biochem* 72:248–254
- Coseteng MY, Lee CY (1987) *J Food Sci* 52:985–989
- Jiménez-Hernández L, Estévez-Hernández O, Hernández-Sánchez M et al (2016) *Colloids Surf A* 489:351–359
- Garmaroudi ZA, Mohammadi MR (2016) *J Am Ceram Soc* 99:167–173
- Swartz HM, Bolton JR, Borg DC (eds) (1972) *Biological applications of electron spin resonance*. Wiley, New York
- Poorakbar E, Shafiee A, Saboury AA et al (2018) *Process Biochem* 71:92–100
- Diñçer A, Becerik S, Aydemir T (2012) *Int J Biol Macromol* 50:815–820
- Aytar BS, Bakir U (2008) *Process Biochem* 43:125–131
- Çakmak R, Topal G, Çınar E (2020) *Appl Biochem Biotechnol* 191:1411–1431
- Arica MY, Bayramoğlu G, Bıçak N (2004) *Process Biochem* 39:2007–2017
- Wu Q, Xu Z, Duan Y et al (2017) *RSC Adv* 7:28114–28123
- Nicolucci C, Rossi S, Menale C et al (2011) *Biodegradation* 22:673–683
- da Silva LV, Tavares AP, Kameda E et al (2013) *Int J Environ Sci* 70:316–326
- Suzuki M, Sugiyama T, Musashi E et al (2010) *J Appl Polym Sci* 118:721–732
- Yamada K, Akiba Y, Shibuya T et al (2005) *Biotechnol Prog* 21:823–829
- Yoshida M, Ono H, Mori Y et al (2001) *Biosci Biotechnol Biochem* 65:1444–1446
- Xu DY, Yang Z (2013) *Chemosphere* 92:391–398
- Bayramoglu G, Akbulut A, Arica MY (2013) *J Hazard Mater* 244:528–536
- Erkmen C, Kurbanoglu S, Uslu B (2020) *Sens Actuators B* 316:128121

Publisher's Note Springer Nature remains neutral with regard to jurisdictional claims in published maps and institutional affiliations.

Authors and Affiliations

Rukiye Yavaşer¹  · Deniz Aktaş Uygun¹  · Arife Alev Karagözler¹ 

Deniz Aktaş Uygun
daktas@adu.edu.tr

Arife Alev Karagözler
akaragozler@adu.edu.tr

¹ Chemistry Department, Faculty of Arts and Sciences, Aydın
Adnan Menderes University, 09010 Aydın, Turkey